ACS APPLIED MATERIALS & INTERFACES

Article

Surface composition of silver nanocubes and their influence on morphological stabilization and catalytic performance in ethylene epoxidation

Shiv Shankar Sangaru, Haibo Zhu, Devon C. Rosenfeld, Akshaya Kumar Samal, Dalaver H. Anjum, and Jean-Marie Basset

ACS Appl. Mater. Interfaces, **Just Accepted Manuscript** • DOI: 10.1021/acsami.5b09927 • Publication Date (Web): 04 Dec 2015

Just Accepted

ACS Publications

ACS Applied Materials & Interfaces is published by the American Chemical Society. 1155 Sixteenth Street N.W., Washington, DC 20036

Surface composition of silver nanocubes and their influence on morphological stabilization and catalytic performance in ethylene epoxidation

Shiv Shankar Sangaru[a, ‡], Haibo Zhu[a, ‡], Devon C. Rosenfeld[b], Akshaya Kumar Samal[a], Dalaver Anjum[c], Jean-Marie Basset[a,*]

[a] *KAUST Catalysis Center, King Abdullah University of Science and Technology, Thuwal, 23955-6900, Kingdom of Saudi Arabia*

[b] *The Dow Chemical Company, 2301 N. Brazosport Blvd., Freeport, TX 77541, USA*

[c] *Imaging and characterization Lab, King Abdullah University of Science and Technology Thuwal, 23955-6900, Kingdom of Saudi Arabia*

KEYWORDS: Silver nanocubes, Polyol method, Catalysis, Ethylene epoxidation.

ABSTRACT: Silver nanocubes with exposed (100) facets are reported to have improved selectivity with respect to their spherical counterparts for ethylene epoxidation. In the present study, we observe that the surface composition of the silver nanocubes have also a critical impact on activity. Detailed investigation of the surface composition of silver nanocubes has been carried out using HRTEM, SEM, EDS, EELS and EFTEM. Surfaces of silver nanocubes are "passivated" by chloride and its removal is essential to achieve any catalytic activity. However, the surface chloride is apparently essential for stabilizing the cubic morphology of the particles. Attempts were made to understand the competing effects of the surface species for retaining the morphology of the nanocubes and on their catalytic activity in ethylene epoxidation.

Introduction:

Metal based heterogeneous catalytic systems have undergone a significant transformation in the past few decades. Historically, catalytic systems have been mainly based on direct incorporation of a specific mass percentage of metal onto a support with appropriate dispersion.[1] Developments in synthetic strategies for making metal nanoparticles have made it possible to further enhance the catalytic activity of a given metal by tuning their size[1] and effectively controlling their shapes with different exposed crystallographic facets.[2-4] Notable examples are syntheses of platinum[5] and palladium[6] nanoparticles of different shapes for different catalytic applications.[2,4] El-Sayed and coworkers demonstrated that Pt tetrahedrons were catalytically more active than Pt cubes for the electron-transfer reaction between hexacyanoferrate(III) and thiosulfate ions.[5] Similarly, palladium nanoparticles of different shape have been applied for Suzuki coupling and alkynol hydrogenation.[6] Shape dependent catalytic performance has also been recently reported for rhodium nanoparticles in a variety of catalytic applications.[7,8] Tetrahexahedral Rh particles with high index surfaces exhibited higher electrocatalytic activity as compared to nanoparticles with other nanostructures.[7] Developments in the field of nanoparticle synthesis has enabled the convenient differentiation between the effect of specific crystallographic planes, size and other features such as active sites at edges and defects on their catalytic activities.

Supported silver catalysts have been well studied for ethylene epoxidation.[9] Recently, Linic et al. reported how silver nanocube (AgNCs) size and shape affected epoxidation performance, demonstrating that AgNCs have enhanced catalytic activity as compared to their spherical counterpart.[10-12] The (100) set of planes that form the external facets of the AgNCs have been shown to be more selective than (111) planes for this reaction. In this report, we have attempted

to further study the structural aspects of AgNCs that influence the catalytic activity of the nanoparticles. Apart from the shape, we found the surface composition of the AgNCs is also critical. We observed that the surface of AgNCs synthesized by a modified polyol method consists predominantly of chloride. Removal of the chloride results in AgNCs that are active for ethylene epoxidation. Using several characterization techniques the surface composition and their morphological stability of the AgNCs were investigated.

Experimental Section:

Silver nitrate (99 %), polyvinylpyrrolidone (PVP) with average $M_W \sim 55{,}000$, and ammonia were all purchased from Sigma. Ethylene glycol (9300-03) and conc. HCl (9530-00) was purchased from J. T. Baker, USA.

AgNCs Synthesis: AgNCs were prepared using a polyol method based on the procedure developed by Xia's group[13] along with modifications reported by Gupta *et al*.[14] Ethylene glycol (15 mL) was heated in argon atmosphere for an hour at 140° C followed by addition of 100 μL of 30 mM HCl in ethylene glycol. After 20 min, 9 mL each of PVP (1.5 mM) and $AgNO_3$ (1.0 mM) in ethylene glycol were added drop-wise using a syringe pump at the rate of 0.75 mL/min. 7 % Oxygen (in Argon) was then bubbled at a rate of 3 mL/min through the solution maintained at 140 °C. The solution started to turn opaque ochre in color indicating formation of AgNCs at around 20 h time, however, the reaction was continued as such for another 6 h and then cooled with an ice bath for further separation of the nanoparticles from the reaction solution by centrifugation. Introduction of oxygen was only crucial during the first few hours of reaction (around 6 h). After the reaction mixture was cooled using an ice bath, excess acetone was added to the reaction vessel followed by centrifugation at 1600×g for 20 min. The settled pellet was

redispersed in deionized water and centrifuged at 1600×g for 1 h in two cycles. Two more cycles of centrifugation were further repeated with redispersion in ethanol. For treatment with aq. NH_4OH, the AgNCs were dispersed in 5 mL deionized water, washed with aq. NH_4OH, agitated and centrifuged prior to their dispersion in ethanol. The AgNCs dispersed in ethanol were used for loading onto alumina support.

Removal of surface chloride: To the above AgNC suspension in water, 4 mL of aq. PVP-55 (10 mg/mL) solution was added and then diluted to 20 mL with water to which 400 μL of aq. NH_4OH (32 %) was added. This solution was agitated at 600 rpm for 2 h. After agitation, the solution was again centrifuged at 3000×g for 1 h followed by redispersion in ethanol. Control experiments were carried out by conducting the aforementioned treatment for 12 h using 1.25 mL of aq. NH_4OH (32 %) in 20 mL of net AgNCs solution.

AgNCs dispersed in ethanol was mixed with dry alumina and agitated at 600 rpm overnight. The alumina supported AgNCs were then separated by mild centrifugation and then dried in vacuum overnight for their subsequent use in catalysis. Efficient adsorption of AgNCs on alumina was only observed when the AgNCs were dispersed in ethanol. SEM imaging was done using SEM Quanta 600 equipped with an EDS system. The specimens for SEM analysis were prepared by drop casting AgNC solution over conducting aluminum tape or by depositing dry alumina supported AgNC catalyst over a conducting carbon tape. While the HRTEM imaging, EELS, and EFTEM analyses were done by using an FEI Company's Titan G2 80-300 CT transmission electron microscope equipped with a charge-coupled device (CCD) camera (model US4000) from Gatan, Inc. TEM-specimens of all samples were prepared by drop casting the AgNC solution over a carbon coated copper grid and dried in the ambient environment. The elemental

mapping with EFTEM imaging analysis was performed with the post-column energy filter from Gatan Inc. of model's Tridiem 863 energy filter equipped on the above-mentioned HRTEM. It should be noted that the so-called jump-ratio method[15] was employed to generate the elemental maps of Cl and Ag. Moreover, the Cl mapping was done using Cl-L2,3 (200 eV) edge and Ag mapping was done using Ag-M4,5 edge (367 eV) were selected to generate the elemental maps of Cl and Ag, respectively. The jump-ratio method, unlike other methods enabled the collection of elemental maps using a minimum electron dose because it requires only a post-edge image and a pre-edge image. The signals were acquired with a slit width of 10 eV energy; the jump ratio method was employed to generate the elemental mapping images in order to reduce the electron dosage over the sample during imaging. Percentage of silver loading was analyzed by ICP-OES technique using a Varian 720-ES instrument. The alumina supported silver catalyst samples were digested with aqua regia (3 parts conc. HCl and 1 part conc. HNO_3) by microwave technique for ICP-OES analysis.

The ethylene epoxidation reaction was carried out in a fixed bed reactor with a PID control system and online GC analysis. 1 g supported Ag catalyst was introduced into the reactor with glass wool as the support. The feed composed of C_2H_4 and O_2 in He was passed through the catalytic bed to perform the catalytic reaction at different conditions. The effect of ratio of O_2 to ethylene on the catalytic performance was performed at 230°C by varying the O_2/C_2H_4 ratio from 0.25 to 4, and the total flow rate was kept at 20 ml/min. To explore relationship between ethylene oxide selectivity and ethylene conversion at 230 °C, the total flow rate (17.8% C_2H_4 and 4.5% O_2 in He) was changed from 10 to 80 mL/min to achieve different levels of conversion and selectivity. The catalytic reaction at different temperatures (200-300 °C) was carried out with an O_2/C_2H_4 ratio of 1:4 (17.8% C_2H_4 and 4.5% O_2 in He) and total flow of 20 ml/min. The test was

performed in the same Ag/Al_2O_3 catalyst by heating it from 200 to 300 °C with a ramp rate of 1°C/minute, and stay at each temperature investigated for 2 hours to collect stable catalytic data. The gas products were analyzed by an on-line Varian 490 micro-GC equipped with TCD detectors and two columns: MolSieve 5Å column (Ar as carrier gas) used to quantify O_2, and a poraPLOT Q column (He as carrier gas) to analyze CO_2, C_2H_4 and C_2H_4O. The ethylene conversion and selectivity to ethylene oxide were calculated on a carbon basis.

Result and discussion:

AgNCs were successfully synthesized by following the polyol method in the presence of HCl developed by Xia's group.[13] Prior to this, attempts were first made to synthesize the AgNCs in the absence of HCl as an additive[16]. However, in our hands this method did not reproducibly form nanoparticles with adequate shape control, and instead produced a mixture of nanoparticle with different shapes.[14] Synthesis in the presence of sodium sulfide/sodium hydrosulfide[17] or bromide source[18] are reported to reproducibly provide AgNCs with good size control, however, the presence of sulfide or bromide on the silver surface was shown to negatively affect epoxidation activity.[13] Therefore, we sought to modify the polyol/HCl method and reproducibly synthesize AgNC with morphology and size control without negatively effecting epoxidation activity.[13] We observed that introduction of an oxygen and argon mixture, as reported by Gooding's group,[14] greatly improved the reproducible synthesis of AgNCs. We also observed that the purity (in terms of trace metal ion contaminants) of all chemicals and cleanliness of all glassware and apparatus employed are critical[14,17]. Additionally, we observed that during the synthesis, introduction of a controlled amount of oxygen was only crucial during the first 6 h of reaction. Figure 1 shows SEM images of AgNCs obtained by this method. The synthesis reproducibly yielded nanoparticles that are almost exclusively nanocubes and are of narrow size

distribution with the average particle size being ~ 125 nm. During the synthesis, the solution goes through a series of color changes from white, faint yellow, colorless to faint brick red and finally opaque ochre as mentioned in previous reports[13] and shown in our supporting information SI-1. The solution color first turns white on addition of the PVP and $AgNO_3$ solutions due to precipitation of AgCl. As the reduction of Ag^+ ions starts, the whitish color begins to turn faint yellow in color (before the addition of silver ions is finished). At this stage, introduction of oxygen to the reaction was found to be crucial for generating AgNCs. A 7 % oxygen in argon mixture was bubbled into the reaction solution at a rate of 2.5 mL/min. Oxygen addition caused the reaction solution to slowly turn colorless and after 2 - 3 h the solution began to develop a very faint brick red coloration and turbidity, which over 6 – 8 h time continues to become more turbid. Continued introduction of oxygen for an additional 10-12 h caused the solution to become an opaque ochre color. Switching the reaction gas from O_2/Ar to pure argon after 6-8 h at the same flow rate accelerated the nanocube growth rate. AgNC yield was unaffected by changing the reaction gas. Apparently, once the nucleation stage is completed and the twinned particles are consumed,[19-23] a moderate increase in growth rate that does not promote fresh nucleation did not seem to affect the yield of cubic particles.

The AgNCs thus synthesized and dispersed in ethanol after separation by centrifugation, as described in the experimental section, were loaded onto α-alumina by simple physical adsorption. However, contrary to our expectation the AgNCs on alumina did not show any catalytic activity towards epoxidation of ethylene (EE) with oxygen. We initially attributed the observed lack of catalytic activity to the silver active sites being blocked by the presence of capping PVP molecules. TGA analysis of the AgNCs under air showed the onset of weight loss at 300 °C. We therefore treated the catalyst with up to 50 % O_2 gas (in He) at 300 °C for 2 h to

remove any organic matter from the surface. However, no improvement in the catalytic activity was observed after such a treatment. Moreover, alumina loaded with PVP capped spherical silver nanoparticles was active for epoxidation under the same testing conditions with selectivity for ethylene oxide (EO) around 45 % (data not shown), consistent with earlier reports.[10] Next, we hypothesized that inactive silver oxide had formed on the AgNC surface. Heating the catalyst under flowing H_2 gas to reduce any surface oxidized silver did not result in epoxidation activity. Even a combination of the two treatments, with the former following the later did not lead to any activity. Considering the additives used during the synthesis, the only remaining additive that could most likely be influencing the activity was chloride. Chloride could possibly form insoluble silver chloride in presence of unreacted silver ions. An early indication of their possible presence was also observed in the XRD pattern of the AgNCs (Figure SI-2). Apart from the usual Bragg reflections at 2θ values matching with bulk *fcc* silver, we observed some very low intensity peaks in the lower 2θ value range between 25° to 35°. Two peaks observed at 27.8° and 32.2° potentially represent the (111) and (200) lattice planes of AgCl. Though this proves the presence of AgCl in our AgNC sample, it does not distinguish between AgCl on AgNC surfaces or in a physical mixture with the AgNCs. To remove chloride we wanted to employ a mild method that avoided harsh conditions such as high temperature in order to maintain AgNC morphology. As aq. NH_4OH solution readily dissolves silver chloride, we expected it would remove chloride from the surface of the AgNCs. The as prepared AgNCs, dispersed in water were treated with 0.64 % aq. NH_4OH solution and later loaded onto α-alumina support. The alumina supported AgNCs (1.44 % Ag as determined by ICP-OES) washed with NH_4OH were active for the ethylene epoxidation reaction. Onset of the epoxidation activity potentially illustrates that chloride is bound to the surface of the AgNCs and inhibits catalysis. Surface

characterization of the AgNCs will be described later. By changing the O_2/C_2H_4 ratio from 0.25 to 4 the ethylene conversion rate in the epoxidation reaction increased from 5 % to nearly 12 % and the corresponding ethylene oxide selectivity increased from 58 to 72 % as shown in Figure 2A. On increasing the contact time by reducing the flow rate from 80 to 10 mL/min at the constant O_2/C_2H_4 ratio of 0.25, ethylene conversion increased from less than 3 % to more than 6 % and selectivity towards ethylene oxide marginally increased from 58 to 62 %. (Figure 2B). Moreover, the conversion and selectivity were observed to be quite stable with respect to the time on stream (Figure 3A). With respect to varying the temperature from 200-300 **°C**, selectivity towards ethylene epoxidation decreased steadily with concomitant increase in conversion (Figure 3B). All these results are consistent with those reported by Linic's group.[10] Use of chloride at ppm level is a common approach to promote selectivity of ethylene epoxidation reaction by blocking the more active sites in order to promote favorable interaction between the oxygen species and ethylene.[24] Presence of excess chloride on the silver surface however was previously reported to deactivate the catalyst.[25] Hence the main objective of this work was to investigate the surface composition of the AgNCs that have been synthesized by the polyol method in the presence of HCl and a controlled amount of oxygen.

To investigate the surface of the AgNCs, we will first compare the SEM images and corresponding EDS of AgNCs before and after treatment with aq. ammonia as shown in Figure 4. One of the striking differences seen between the as prepared AgNCs and the two sets of AgNCs treated with aq. ammonium hydroxide is that the as prepared AgNCs have well defined sharp edges, and post treatment the AgNCs have more rounded edges. Incidentally, this also coincides with the reports by Xia's group where the AgNCs synthesized in presence of HCl[13] have comparatively sharp edges with respect to those synthesized in absence of it.[16] EDS

measurements revealed that the amount of chloride decreased on treatment with aq. NH_4OH though it was not completely eliminated (Figure 4). However, the indicated residual percentage of chloride present after NH_4OH washing is less than 1 % which is close to the detection limit of the EDS. Moreover, the Ag L1 line at 2.633 eV has an overlap with the Cl Kα lines; hence these results best serve as indicator of decreasing chloride concentration after washing with NH_4OH. Interestingly, when the AgNCs were treated with more concentrated ammonium hydroxide solutions (> 1 %), it is observed that, along with a decrease in the percentage of chloride in the sample an almost complete deformation of the AgNCs to near spherical shape occurs. Such behavior was clearly observed when using 2-5 % aq. NH_4OH solutions. On using higher percentage of aq. NH_4OH a spontaneous destabilization of solution into non-dispersible gray-black precipitates was observed. Similar, nanocube morphology deformation was observed when the AgNCs were treated with 0.64 % aq. NH_4OH solution for more than 12 h. The effect of treatment with aq. NH_4OH was in fact not as mild as we expected. It may however be noted that though aggressive treatment with aq. NH_4OH solution apparently decreased the relative amount of detected chloride in the sample, we did not observe any complete removal of chloride in these samples. Unlike the progressive etching of the AgNCs observed in the presence of H_2O_2, prolonged treatment with concentrated aq. NH_4OH changed the morphology of the AgNCs through deformation of the cubic metallic part of the morphology.[26] As shown in supporting information SI-3, the catalytic reaction performed on these deformed nanoparticles supported on α-A_2O_3 resulted in a lower selectivity (47%) than that (59%) observed with particles which retained their cubic morphology. Therefore, the cubic shape of Ag rather than Cl remaining in the sample is a crucial factor contributing to the enhanced selectivity towards the formation of ethylene oxide. However, the presence of chloride on the nanoparticle surface stabilizes the

cubic structure of the silver nanoparticles bound by the (100) set of facets. However, such a conclusion requires direct evidence proving the presence of chloride on the surface of the nanoparticle. Such information could only be collected by measuring chloride on individual particles rather than analyzing the bulk. We therefore analyzed the AgNCs with HRTEM. Figure 5 shows a representative HRTEM image of AgNCs that clearly show a distinct layer approximately 2.3 nm thick on the AgNC surface. The lattice spacing in the bulk of the nanoparticle is *ca*. 2.02 Å and corresponds to the (200) set of lattice planes of Ag with fcc crystalline structure. The distinct layer at the AgNC surface also has a lattice like structure, however it does not have perfectly parallel planes with uniform spacing as observed for the bulk Ag (200) set of planes (Figure 5C). The average spacing was 2.73 Å which is close to the AgCl (200) set of planes with a d-spacing of 2.77 Å. Attempts were made to identify the composition of this outer layer by acquiring EDS selectively at the surface, however the particles were not stable under the high intensity focused beam hence data could not be acquired. The beam damage to a single AgNC particle is reported in the supporting information SI-4. HRTEM images of AgNCs treated with aq. NH_4OH are shown in Figure 6. In figure 6A the aq. NH_4OH treated AgNCs, though being essentially cubic in morphology, have rounded edges as also observed by SEM. Images obtained at higher magnification (Figure 6B and inset therein) showed these particles do not have the distinct layer on the surface that was observed on the untreated AgNCs (Figure 5C). EELS spectra collected from both untreated AgNCs and those treated with aq. NH_4OH are shown in Figure 6C. A distinct edge at 200 eV can be observed for untreated AgNCs (curve a) and matches well with the reported values[27]. In comparison, AgNCs treated with aq. NH_4OH solution do not exhibit this signal (curve b), providing unambiguous confirmation of the presence of chloride in the outer layer of the untreated nanocubes. While

EELS measurements proved the presence of chloride in the outer layer of the untreated AgNCs, the most convincing evidence of the presence of chloride in the outer surface layer on these AgNCs was obtained with the EFTEM. This technique was especially suitable for analyzing the AgNCs as the imaging could be done with much less electron beam dose per unit area thereby preventing any damage to the particle during imaging. In Figure 7 A-C, panel A shows the bright field image of AgNCs on which elemental mapping was carried out. Figure 7B is an image of AgNCs showing the elemental mapping acquired from the Cl-$L_{2,3}$ edge (200 eV). A distinct signal of chlorine from the nanoparticle with respect to the background and its uniform intensity over the cubic particles with more intense signal at the boundaries is observed. In Figure 7C an elemental map formed by combining images acquired from the Cl $L_{2,3}$ edge (green) and Ag-$M_{4,5}$ edge (367 eV; red) signals is shown. This image not only confirms the presence of Cl in the sample but also clearly demonstrates that the chloride is distributed over the surface of all the observed particles. The EFTEM images in Figure 7 D-F are from the AgNCs after treatment with aq. NH_4OH and clearly demonstrate the change in chloride coverage on the surface. In panel E the elemental map corresponding to the AgNCs shown in the bright field image (panel D) was acquired using Cl $L_{2,3}$ edge and only a weak signal from Cl is visible from the particle. In Figure 7F the elemental map formed by combining images separately acquired from chlorine $L_{2,3}$ edge (green) and silver $M_{4,5}$ edge (red) clearly show that the AgNC surface consists of mainly silver with a significantly lower amount of chloride. In combination with XRD and HRTEM analysis it can be concluded that the chloride is deposited in the form of ordered layers of AgCl on the surface of the AgNCs. The structure of the chloride layer formed on the metallic Ag surface by externally introducing chlorine species is reportedly different from bulk AgCl lattice formed from Ag^+ and Cl^- ions[28]. Such structural differences between an AgCl like structure on Ag (100)

facets in our case and the usual Cl species included on metallic silver surface as a promoter could possibly be the reason behind the lack of epoxidation activity of the as prepared AgNCs in the present case. Additionally, the catalytically active inclusion of subsurface Cl species promoting ethylene epoxidation selectivity is believed to be only kinetically favored as opposed to the thermodynamically favored AgCl layer.[29] Hence, in the synthesis conditions followed here only a thermodynamically stable AgCl is formed on the core metallic AgNC surface.

In terms of the catalytic activity, it is also known that the improvement in selectivity in ethylene epoxidation from chloride addition is accompanied by reduced activity.[30] The increase in selectivity is attributed to the nonselective active sites being blocked by Cl species, which additionally help in improving the electrophilicity of the neighboring adsorbed oxygen species due to their own electronegativity. However, the poisoning of the catalyst due to excess accumulation of Cl from the feed gas is mitigated by its removal via the stripping reaction with ethylene.[30] In the present case, the AgNCs are already deactivated by the presence of surface chloride, and in-situ pretreatments did not help in inducing any activity. Further, prolonged heating for nearly 40 h during AgNC synthesis to allow complete reduction of silver ions too did not result in any active catalyst. Hence, the observed surface chloride layer cannot be attributed to any surface deposition due to premature termination of the reaction preventing complete reduction of silver. The thermodynamic factors favoring the stable adsorption of Cl on silver surface[29,31] and epitaxial deposition of AgCl on Ag surface[32] could possibly be preventing the complete reduction of silver ions under the reaction conditions followed here.

We also explored the thermal stability of the NH_4OH treated AgNCs. When the epoxidation reaction was carried out at temperatures below 230 °C, the AgNCs retained their cubic shape for even up to 6 days. At 230 °C a partial deformation of the AgNCs were observed (Figure SI-5).

However, when epoxidation was carried out above 230 °C, the AgNCs lost their cubic morphology and became spherical. As shown in Figure 8 the AgNCs were observed to attain spherical morphology after 2 days of reaction at 240 °C. We hypothesized that this shape change was caused by surface melting/reconstruction of the AgNC forming spheres. To observe the melting of the AgNCs, TEM was done with in-situ heating by using a holder equipped with a heating stage. Although the AgNCs were heated up to 410 °C under vacuum, which was beyond the tested temperature range for the ethylene epoxidation reaction, no melting was observed and the post heating micrographs in Figure SI-6 show the cubic morphology remained intact. Hence it is very likely that the observed deformation of the particles during the catalytic reaction is due to the exothermicity of the reaction at the surface. In the epoxidation reaction, EO formation is reported to be moderately exothermic (-105 kJ/mol), however the complete oxidation of ethylene and EO to CO_2 is strongly exothermic (-1,327 and -1,223 kJ/mol, respectively)[30, 33]. From catalytic activity data shown in Figure 3B with respect to the variation in temperature, it could be possible that around 230 °C when the selectivity drops below 60 % the heat contribution from the highly exothermic path of complete combustion becomes significant enough at these temperatures to effect morphological deformation, which favors formation of a thermodynamically more stable near spherical shape. Additionally, this could also be assisted by the surface reconstruction that is proposed to occur after the adsorption of oxygen and ethylene interaction in the oxometallacycle (OMC) pathway.[24]

In conclusion, a modified polyol method in the presence of HCl and 7 % oxygen in argon results in the reproducible synthesis of AgNCs of a single morphology and narrow size distribution. The addition of HCl advantageously stabilizes the nanocubes during formation, unfortunately the presence of chloride results in the formation of an outer layer of AgCl that

passivates the catalytic activity of the AgNCs towards ethylene epoxidation. The lack of epoxidation activity is potentially linked to the structural difference between the surface AgCl layer deposited during synthesis in the presence of HCl and as the adsorbed chloride deposited on the active silver surface when introduced as a promoter. Removal of the surface chloride by washing the AgNCs with an aq. NH_4OH solution deforms the cubic morphology by rounding the edges and upon longer NH_4OH exposure changes to a spherical shape. Mild treatment with aq. NH_4OH is essential to retain the cubic shape with minimal deformation. The AgNCs dispersed on alumina were only active for ethylene epoxidation if they were first treated with aq. NH_4OH to remove the chloride bound to the nanocube surface. Additionally, the AgNCs also undergo deformation when the ethylene epoxidation reaction is carried out at temperatures above 230 °C, whereas under vacuum no morphological deformation is observed within these temperature ranges. The surface distribution of the AgCl layer on AgNPs and its successful removal by aq. NH_4OH treatment to activate the catalyst was confirmed by detailed characterization using HRTEM, EELS and EFTEM imaging.

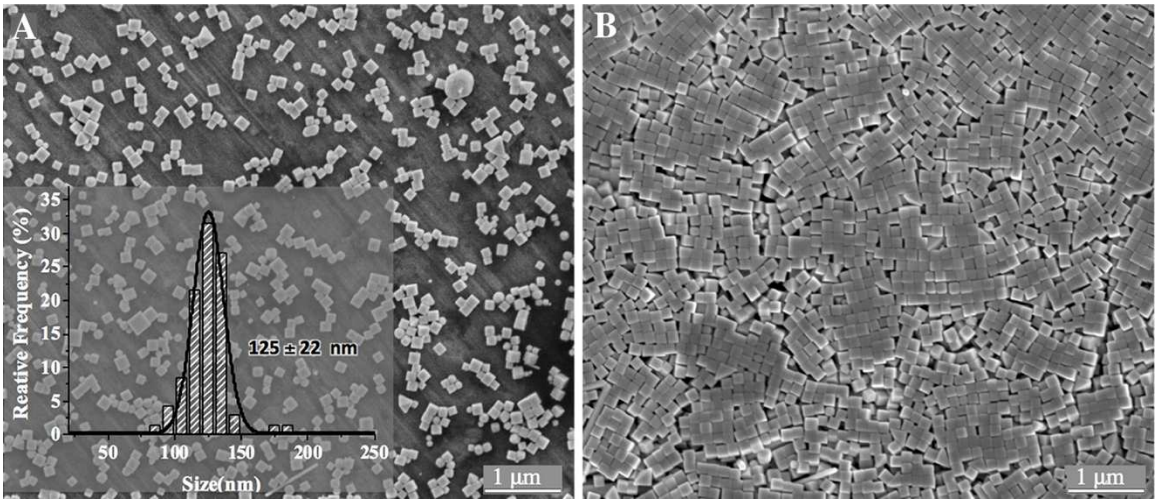

Figure 1: SEM Images of AgNCs synthesized by polyol method in presence of HCl and 7 % oxygen in argon. The inset in panel A shows the histogram of particles size distribution of AgNCs fitted with a Gaussian curve.

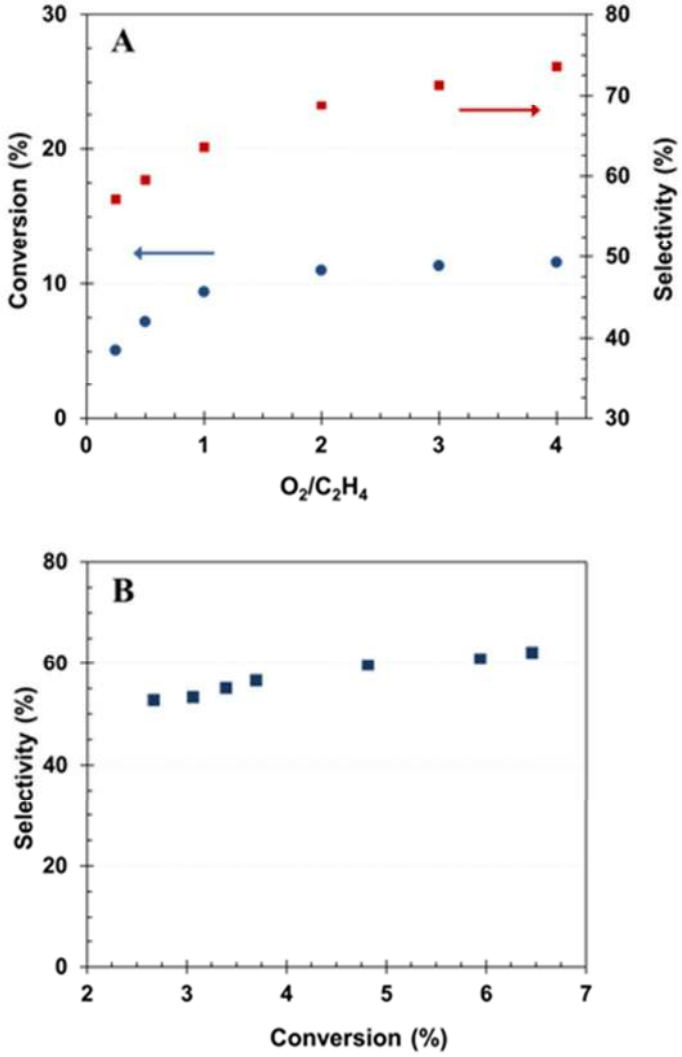

Figure 2: A) Plot of conversion (blue circles) and selectivity (Red squares) as function of the ratio of O_2 : ethylene. B) Relation between selectivity and conversion measured by changing the contact time by decreasing the flow rate of feed gas from 80 to 10 mL/min.

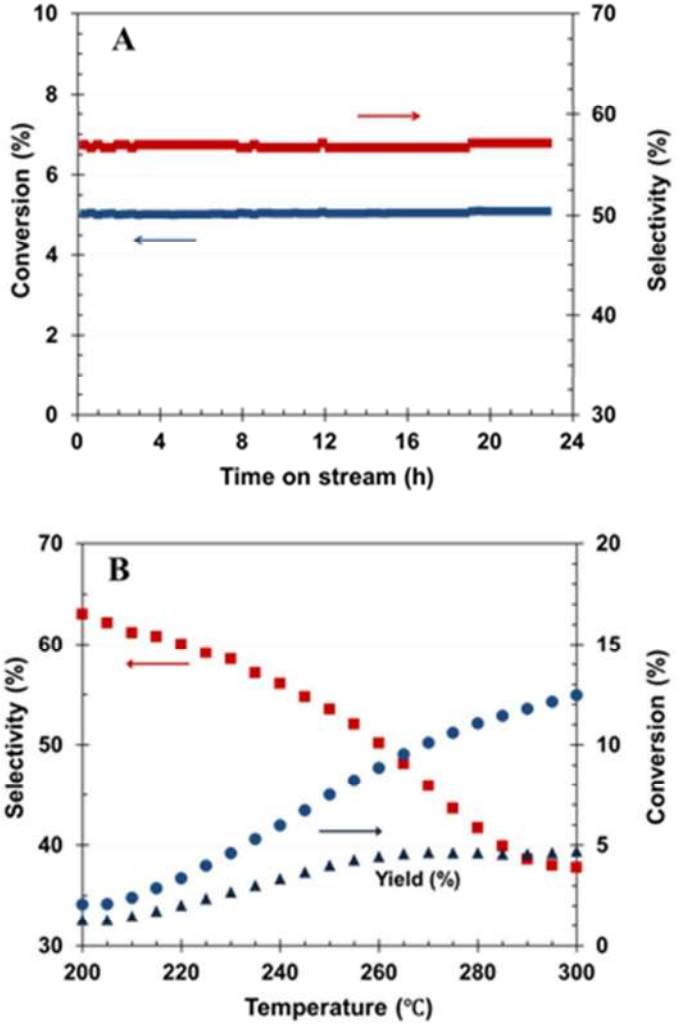

Figure 3: A) Conversion of ethylene and selectivity towards ethylene epoxide formation as a function of time on stream. The reaction was carried out at 230 °C with O_2/C_2H_4 ratio of 1:4 and total flow rate of 20 ml/minute. The curves with left and right arrows correspond to left axis for conversion values and right axis for selectivity values, respectively. B) Plot of selectivity towards EO (red squares) and conversion of EE (blue circles) and yield (blue triangles) with respect to temperature. The associated arrows for each curves indicate their corresponding axes.

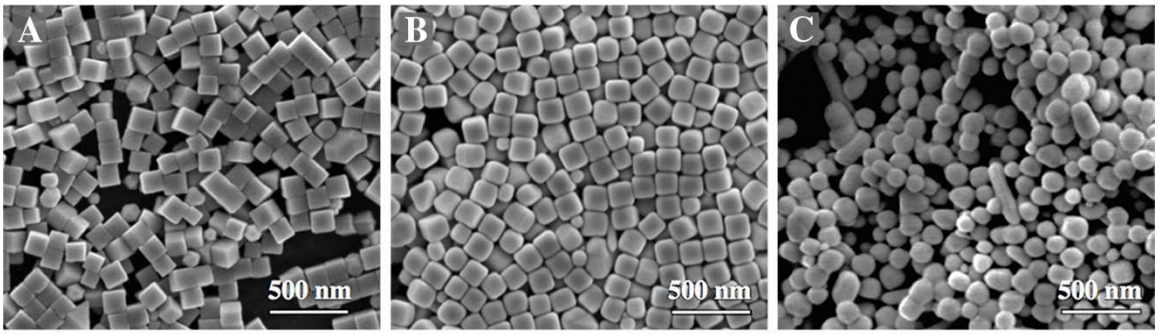

EDS

Element	Wt%	At%
ClK	00.64	01.93
AgL	99.36	98.07

Element	Wt%	At%
ClK	00.26	00.80
AgL	99.74	99.20

Element	Wt%	At%
ClK	00.16	00.47
AgL	99.84	99.53

Figure 4: SEM image of AgNCs (A) as prepared AgNCs before treatment with aq. NH_4OH, (B) after mild treatment with aq. NH_4OH (0.64 %) for 2 h and (C) after treatment with 2 % NH_4OH for 12 h.

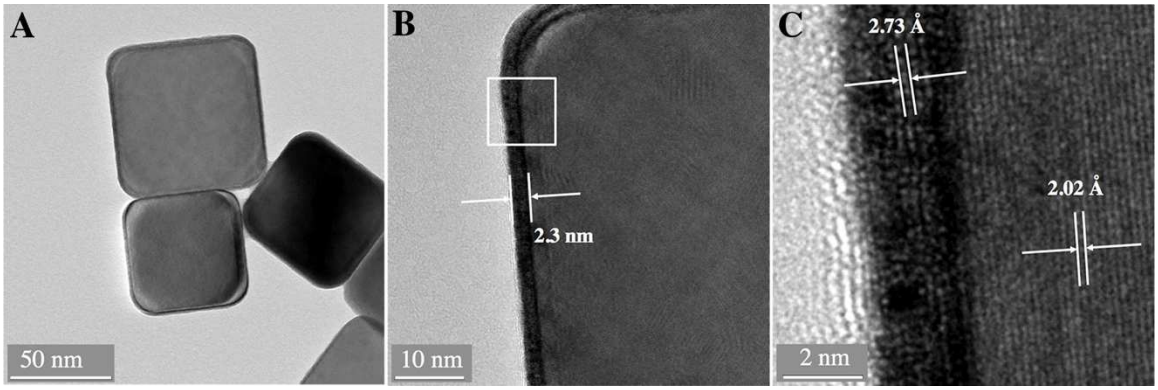

Figure 5: (A) Low magnification BF-TEM micrograph of as prepared AgNCs before treatment with aq. NH_4OH, (B) Higher magnification HRTEM micrograph of the top AgNC shown in panel A, and (C) enlarged image of the section indicated by a white box in panel B.

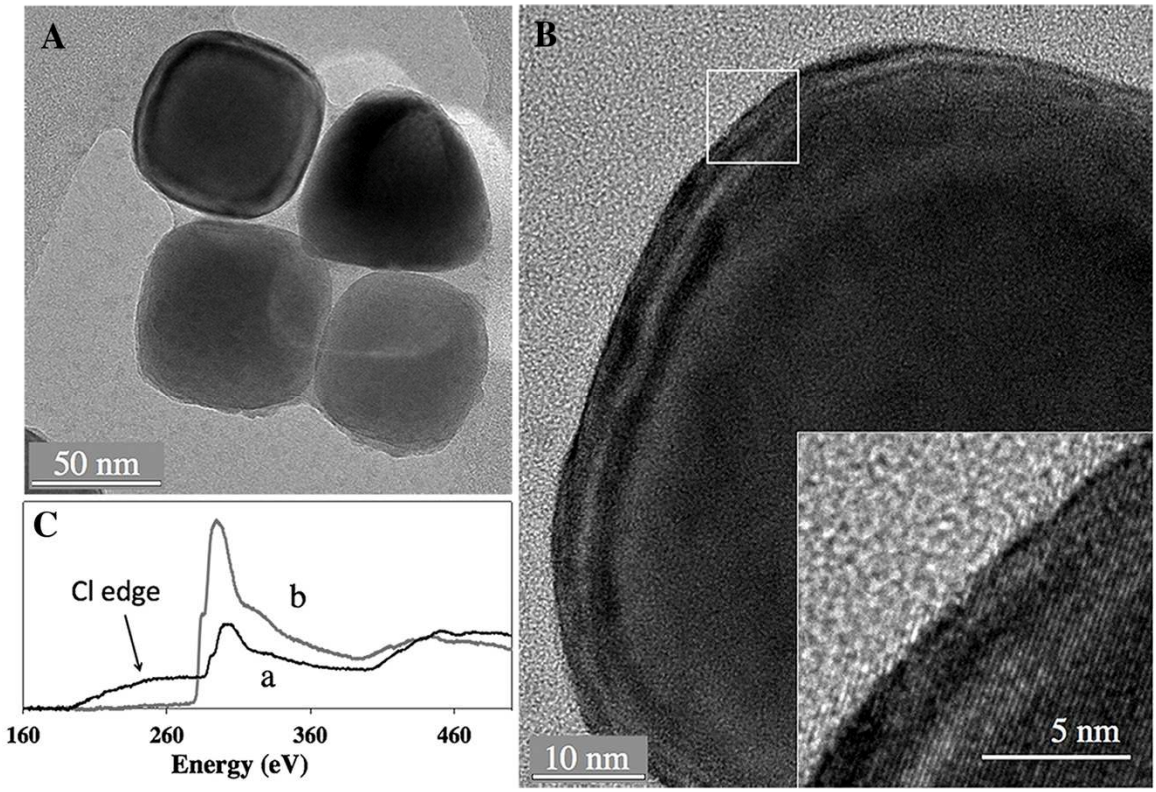

Figure 6: (A) BF-HRTEM image of AgNCs after treatment with 0.64 % aq. NH_4OH for 2 h, (B) Higher magnification HRTEM micrograph of top left AgNC shown in image A and the inset is an enlarged section of the image enclosed by white square. (C) EELS spectra from untreated AgNC (curve a) and AgNCs treated with aq. NH_4OH (curve b) shown in image of Figure 5B and Figure 6B.

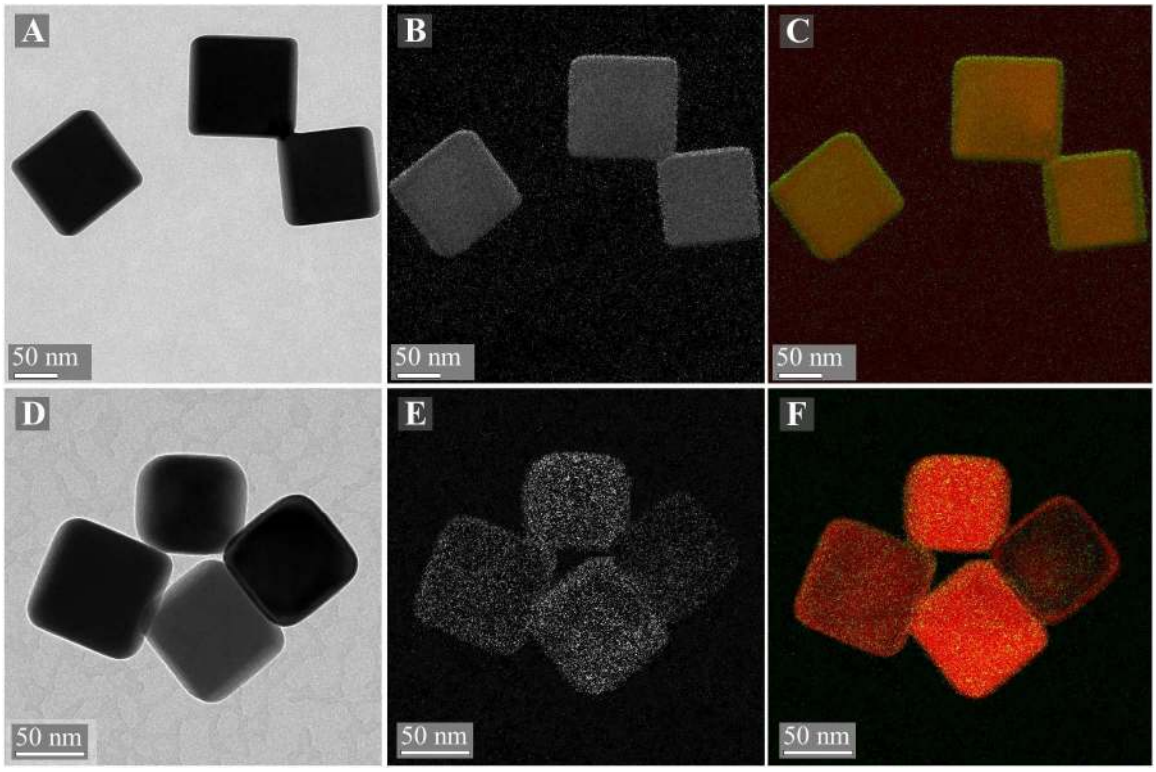

Figure 7: (A) Filtered BF-TEM micrograph of untreated AgNCs (B) Cl elemental map of corresponding to AgNCs shown in panel A acquired from the Cl $L_{2,3}$ energy edge (200 eV), (C) RGB map of Cl and Ag from AgNCs shown in panel A formed by combining EFTEM image from Cl (green) in panel B with similar map acquired from Ag $M_{4,5}$ energy edge at 367 eV (red). D) Filtered BF-TEM micrograph of AgNCs treated with aq. NH_4OH, (E) Elemental map of Cl from AgNCs shown in panel D acquired from the Cl $L_{2,3}$ energy edge (200 eV), (F) RGB map of AgNCs shown in panel D formed by combining map from Cl (green) in panel E with a similar map acquired from Ag $M_{4,5}$ energy edge at 367 eV (red).

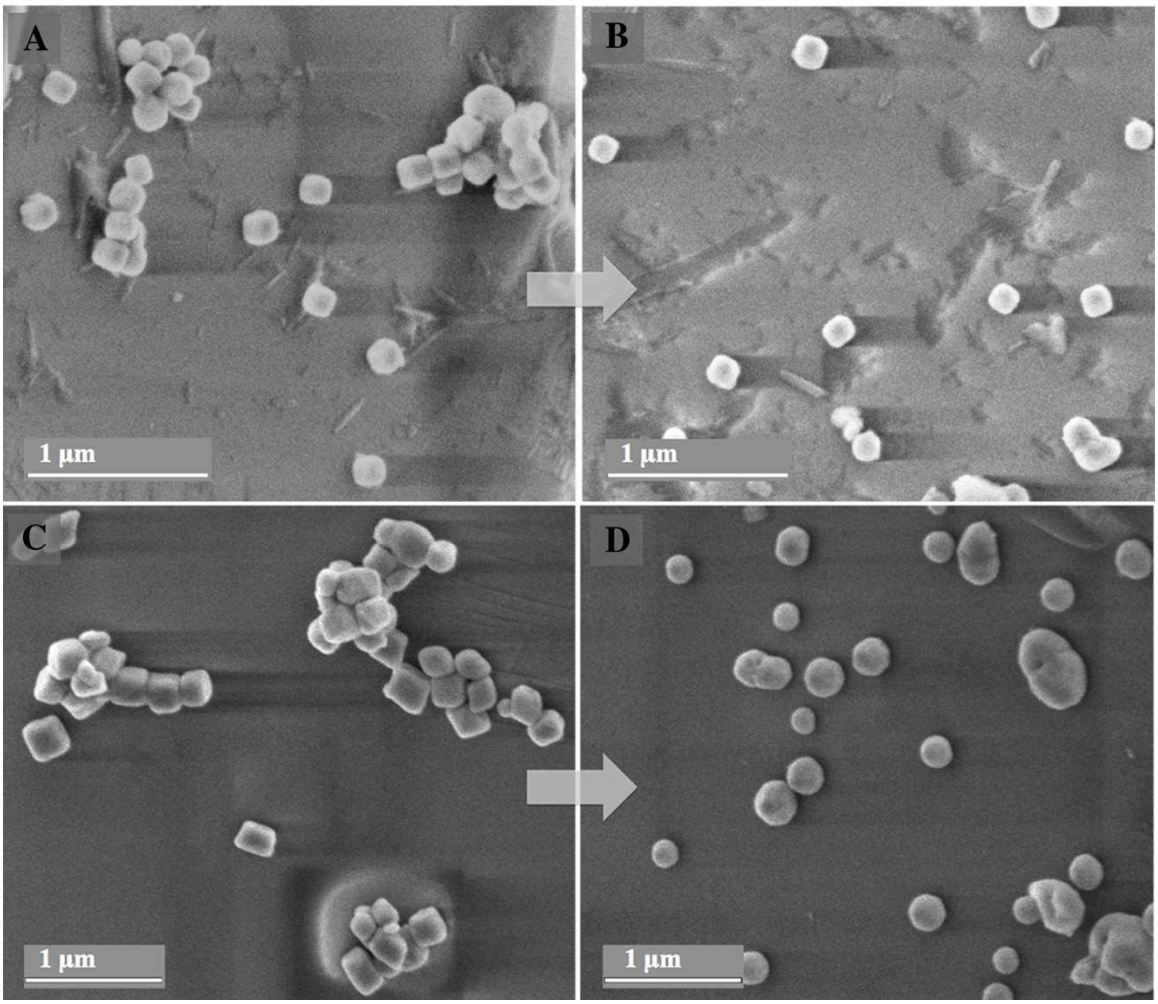

Figure 8: (A) and (C) SEM images of the α-alumina supported AgNC catalyst before using it for EE epoxidation reaction. (B) SEM of the catalyst shown in image A after using it for 6 days for catalyzing the EE epoxidation reaction carried out at 200 °C in a flow reactor. (D) SEM of the catalyst shown in image C after using it for 2 days for catalyzing the EE epoxidation reaction carried out at 240 °C in a flow reactor. The AgNCs were all treated with 0.64 % aq. NH_4OH for 2 h before supporting them on α-alumina.

AUTHOR INFORMATION

Corresponding Author

*Jean-Marie Basset, email: jeanmarie.basset@kaust.edu.sa

Author Contributions

‡Shiv Shankar Sangaru and Haibo Zhu contributed equally. The manuscript was written through contributions of all authors. All authors have given approval to the final version of the manuscript.

Funding Sources

The work presented here was funded by The Dow Chemical Company.

ACKNOWLEDGMENT

SSS and HZ acknowledge the financial support received from The Dow Chemical for the work presented in this manuscript.

ABBREVIATIONS

AgNC, silver nanocubes; HRTEM, High resolution transmission electron microscopy; SEM, Scanning electron microscopy; EDS, energy dispersive X-ray spectroscopy; EELS, electron energy loss spectroscopy; EFTEM, energy filtered transmission electron microscopy; PVP, Polyvinylpyrrolidone; EE, ethylene; EO ethylene epoxide.

REFERENCES

(1) Bukhtiyarov, V. I.; Prosvirin, I. P.; Kvon, R. I.; Goncharova, S. N.; Bal'zhinimaev, B. S. XPS Study of the Size Effect in Ethene Epoxidation on Supported Silver Catalysts. *J. Chem. Soc., Faraday Trans.* **1997***, 93,* 2323-2239.

(2) Zaera, F. Shape-Controlled Nanostructures in Heterogeneous Catalysis. *ChemSusChem* **2013**, *6*, 1797-1820.

(3) Narayanan, R.; El-Sayed, M. A. Catalysis with Transition Metal Nanoparticles in Colloidal Solution: Nanoparticle Shape Dependence and Stability. *J. Phys. Chem. B* **2005**, *109*, 12663-12676.

(4) Ruditskiy, A.; Choi, S.-I.; Peng, H.-C.; Xia, Y. Shape-Controlled Metal Nanocrystals for Catalytic Applications. *MRS Bull.* **2014**, *39*, 727-737.

(5) Narayanan, R.; El-Sayed, M. A. Shape-Dependent Catalytic Activity of Platinum Nanoparticles in Colloidal Solution. *Nano Lett.* **2004**, *4*, 1343-1348.

(6) Zhang, H.; Jin, M.; Xiong, Y.; Lim, B.; Xia, Y. Shape-Controlled Synthesis of Pd Nanocrystals and Their Catalytic Applications. *Acc. Chem. Res.* **2012**, *46*, 1783-1794.

(7) Yu, N.-F.; Tian, N.; Zhou, Z.-Y.; Huang, L.; Xiao, J.; Wen, Y.-H.; Sun, S.-G. Electrochemical Synthesis of Tetrahexahedral Rhodium Nanocrystals with Extraordinarily High Surface Energy and High Electrocatalytic Activity. *Angew. Chem. Int. Ed.* **2014**, *53*, 5097-5101.

(8) Zhang, Y.; Grass, M. E.; Kuhn, J. N.; Tao, F.; Habas, S. E.; Huang, W.; Yang, P.; Somorjai, G. A. Highly Selective Synthesis of Catalytically Active Monodisperse Rhodium Nanocubes. *J. Am. Chem. Soc.* **2008**, *130*, 5868-5869.

(9) Ozbek, M. O.; Onal, I.; van Santen, R. A. Why Silver is the Unique Catalyst for Ethylene Epoxidation. *J. Catal.* **2011**, *284*, 230-235.

(10) Christopher, P.; Linic, S. Shape- and Size-Specific Chemistry of Ag Nanostructures in Catalytic Ethylene Epoxidation. *ChemCatChem* **2010**, *2*, 78-83.

(11) Linic, S.; Christopher, P. Overcoming Limitation in the Design of Selective Solid Catalysts by Manipulating Shape and Size of Catalytic Particles: Epoxidation Reactions on Silver. *ChemCatChem* **2010**, *2*, 1061-1063.

(12) Christopher, P.; Linic, S. Engineering Selectivity in Heterogeneous Catalysis: Ag Nanowires as Selective Ethylene Epoxidation Catalysts. *J. Am. Chem. Soc.* **2008**, *130*, 11264-11265.

(13) Im, S. H.; Lee, Y. T.; Wiley, B.; Xia, Y. Large-Scale Synthesis of Silver Nanocubes: The Role of HCl in Promoting Cube Perfection and Monodispersity. *Angew. Chem. Int. Ed.* **2005**, *44*, 2154-2157.

(14) Gupta, B.; Rouesnel, W.; Gooding, J. J. The Role of Oxygen in Synthesizing Monodisperse Silver Nanocubes. *Aus. J. Chem.* **2011**, *64*, 1488-1493.

(15) Egerton, R. F. Transmission Electron Energy Loss Spectrometry in Materials Science and The EELS Atlas. *Wiley-VCH Verlag GmbH & Co. KGaA*, **2005**, 21-47.

(16) Sun, Y.; Xia, Y. Shape-Controlled Synthesis of Gold and Silver Nanoparticles. *Science* **2002**, *298*, 2176-2179.

(17) Skrabalak, S. E.; Au, L.; Li, X.; Xia, Y. Facile Synthesis of Ag Nanocubes and Au Nanocages. *Nat. Protocols* **2007**, *2*, 2182-2190.

(18) Yu, D.; Yam, V. W.-W. Controlled Synthesis of Monodisperse Silver Nanocubes in Water. *J. Am. Chem. Soc.* **2004**, *126*, 13200-13201.

(19) Wiley, B.; Herricks, T.; Sun, Y.; Xia, Y. Polyol Synthesis of Silver Nanoparticles: Use of Chloride and Oxygen to Promote the Formation of Single-Crystal, Truncated Cubes and Tetrahedrons. *Nano Lett.* **2004**, *4*, 1733-1739.

(20) Long, R.; Zhou, S.; Wiley, B. J.; Xiong, Y. Oxidative Etching for Controlled Synthesis of Metal Nanocrystals: Atomic Addition and Subtraction. *Chem. Soc. Rev.* **2014**, *43*, 6288-6310.

(21) Taguchi, A.; Fujii, S.; Ichimura, T.; Verma, P.; Inouye, Y.; Kawata, S. Oxygen-Assisted Shape Control in Polyol Synthesis of Silver Nanocrystals. *Chem. Phys. Lett.* **2008**, *462*, 92-95.

(22) Chang, S.; Chen, K.; Hua, Q.; Ma, Y.; Huang, W. Evidence for the Growth Mechanisms of Silver Nanocubes and Nanowires. *J. Phys. Chem. C* **2011**, *115*, 7979-7986.

(23) Wiley, B.; Sun, Y.; Mayers, B.; Xia, Y. Shape-Controlled Synthesis of Metal Nanostructures: The Case of Silver. *Chem. Eur. J.* **2005,** *11*, 454-463.

(24) Özbek, M. O.; Önal, I.; van Santen, R. A. Chlorine and Caesium Promotion of Silver Ethylene Epoxidation Catalysts. *ChemCatChem* **2013**, *5*, 443-451.

(25) Lambert, R. M.; Cropley, R. L.; Husain, A.; Tikhov, M. S. Halogen-Induced Selectivity in Heterogeneous Epoxidation is an Electronic Effect-Fluorine, Chlorine, Bromine and Iodine in the Ag-Catalysed Selective Oxidation of Ethene. *Chem. Commun.* **2003**, 1184-1185.

(26) Mulvihill, M. J.; Ling, X. Y.; Henzie, J.; Yang, P. Anisotropic Etching of Silver Nanoparticles for Plasmonic Structures Capable of Single-Particle SERS. *J. Am. Chem. Soc.* **2010**, *132*, 268-274.

(27) Leapman, R. *Transmission Electron Energy Loss Spectrometry in Materials Science and The EELS Atlas*, Wiley-VCH Verlag GmbH & Co. KGaA: 2005, 49-96.

(28) Andryushechkin, B. V.; Cherkez, V. V.; Gladchenko, E. V.; Zhidomirov, G. M.; Kierren, B.; Fagot-Revurat, Y.; Malterre, D.; Eltsov, K. N. New Insight into the Structure of Saturated Chlorine Layer on Ag(1 1 1): LT-STM and DFT Study. *Appl. Surf. Sci.* **2013**, *267*, 21-25.

(29) Gava, P.; Kokalj, A.; de Gironcoli, S.; Baroni, S. Adsorption of Chlorine on Ag(111): No Subsurface Cl at Low Coverage. *Phys. Rev. B* **2008**, *78*, 165419-165434.

(30) Özbek, M. O.; van Santen, R. A. The Mechanism of Ethylene Epoxidation Catalysis. *Catal. Lett.* **2013**, *143*, 131-141.

(31) Iski, E. V.; El-Kouedi, M.; Calderon, C.; Wang, F.; Bellisario, D. O.; Ye, T.; Sykes, E. C. H. The Extraordinary Stability Imparted to Silver Monolayers by Chloride. *Electrochim. Acta* **2011**, *56*, 1652-1661.

(32) Andryushechkin, B. V.; Eltsov, K. N.; Shevlyuga, V. M.; Tarducci, C.; Cortigiani, B.; Bardi, U.; Atrei, A. Epitaxial Growth of AgCl Layers on the Ag(100) Surface. *Surf. Sci.* **1999**, *421*, 27-32.

(33) Kestenbaum, H.; Lange de Oliveira, A.; Schmidt, W.; Schüth, F.; Ehrfeld, W.; Gebauer, K.; Löwe, H.; Richter, T.; Lebiedz, D.; Untiedt, I.; Züchner, H. Silver-Catalyzed Oxidation of Ethylene to Ethylene Oxide in a Microreaction System. *Ind. Eng. Chem. Res.* **2002**, *41*, 710-719.

Unraveling AgCl surface layer for the stabilization of silver nanocubes

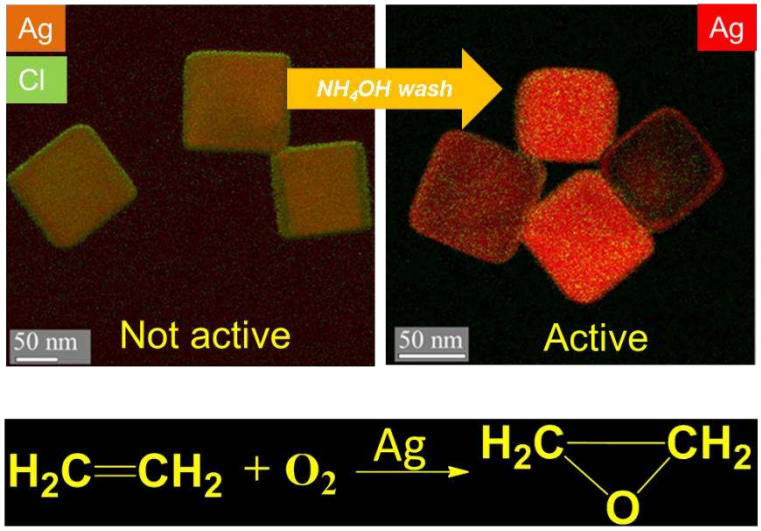

The surface composition of the silver nanocubes synthesized from a polyol method in the presence of HCl, has been systematically studied by using HRTEM, SEM, EDS, EELS and EFTEM techniques.